

NIN is essential for development of symbiosomes, suppression of defence and premature senescence in *Medicago truncatula* nodules

Jieyu Liu¹ , Menno Rasing¹ , Tian Zeng¹ , Joël Klein¹ , Olga Kulikova¹  and Ton Bisseling^{1,2} 

¹Laboratory of Molecular Biology, Department of Plant Sciences, Graduate School Experimental Plant Sciences, Wageningen University & Research, Wageningen 6708 PB, the Netherlands;

²Beijing Advanced Innovation Center for Tree Breeding by Molecular Design, Beijing University of Agriculture, Beijing 102206, China

Summary

Author for correspondence:

Ton Bisseling

Email: ton.bisseling@wur.nl

Received: 11 September 2020

Accepted: 30 November 2020

New Phytologist (2021) 230: 290–303

doi: 10.1111/nph.17215

Key words: defence, early senescence, *Medicago truncatula*, NIN (NODULE INCEPTION), nodule development, symbiosome.

- NIN (NODULE INCEPTION) is a transcription factor that plays a key role during root nodule initiation. However, its role in later nodule developmental stages is unclear.
- Both NIN mRNA and protein accumulated at the highest level in the proximal part of the infection zone in *Medicago truncatula* nodules. Two *nin* weak allele mutants, *nin-13/16*, form a rather normal nodule infection zone, whereas a fixation zone is not formed. Instead, a zone with defence responses and premature senescence occurred and symbiosome development gets arrested.
- Mutations in *nin-13/16* resulted in a truncated NIN lacking the conserved PB1 domain. However, this did not cause the nodule phenotype as *nin* mutants expressing *NIN_{ΔPB1}* formed wild-type-like nodule. The phenotype is likely to be caused by reduced *NIN* mRNA levels in the cytoplasm. Transcriptome analyses of *nin-16* nodules showed that expression levels of defence/senescence-related genes are markedly increased, whereas the levels of defence suppressing genes are reduced. Although defence/senescence seems well suppressed in the infection zone, the transcriptome is already markedly changed in the proximal part of infection zone.
- In addition to its function in infection and nodule organogenesis, NIN also plays a major role at the transition from infection to fixation zone in establishing a functional symbiosis.

Introduction

Legumes have the ability to establish a root nodule symbiosis with bacteria belonging to different genera collectively named rhizobia. Rhizobia are hosted inside specialised nodule cells where they are able to reduce atmospheric nitrogen into ammonia. Root nodule formation involves two main processes, infection and nodule organogenesis (Oldroyd & Downie, 2008). Infection starts in root hairs with the formation of tube-like structures called infection threads by which bacteria enter root cells (Oldroyd *et al.*, 2011). Nodule organogenesis begins with mitotic reactivation of fully differentiated root cells leading to the formation of a nodule primordium (Xiao *et al.*, 2014). NIN (NODULE INCEPTION) is a key transcription factor that is essential for both processes (Schauser *et al.*, 1999; Marsh *et al.*, 2007). Weak alleles of *nin* have been identified that allow the formation of nodules (Pislaru *et al.*, 2012; Veerappan *et al.*, 2016). These nodules are small and do not fix nitrogen, suggesting that NIN also plays a role at later stages of nodule development. However, it is not clear in which nodule developmental process NIN is involved. Here we studied the role of NIN during later nodule developmental stages in *Medicago truncatula* (Medicago).

At the start of nodulation, *NIN* is transcriptionally induced upon perception of rhizobia secreted lipo-chito-oligosaccharides, called Nod factors (NF). NF activate a signalling pathway that is shared with the more ancient arbuscular mycorrhizal symbiosis. NIN is the first induced transcription factor that distinguishes the rhizobium activated responses from that of arbuscular mycorrhizae (Oldroyd, 2013). NIN is not only essential for nodulation in legumes, but also in actinorhizal(-like) plants such as *Casuarina* and *Parasponia* (Clavijo *et al.*, 2015; Bu *et al.*, 2020). In both legumes as well as actinorhizal plants, *NIN* is nodule specifically expressed (Schauser *et al.*, 1999; Marsh *et al.*, 2007; Clavijo *et al.*, 2015; Bu *et al.*, 2020). During nodule initiation in legumes, *NIN* is induced in the epidermis, where it is required for infection thread formation (Vernié *et al.*, 2015). In Medicago, *NIN* is also induced in the pericycle and this marks the start of nodule primordium formation, after which the expression of *NIN* extends to the dividing cortical cells (Liu *et al.*, 2019b).

Medicago forms indeterminate nodules that have a zonation representing successive developmental stages (Vasse *et al.*, 1990). At the apex there is a meristem that continuously adds cells to nodule tissues. Proximal to the meristem is the infection zone, where cells are penetrated by infection threads from which

rhizobia are released. During release, bacteria become surrounded by a plant-derived membrane, these organelle-like structures are called symbiosomes (Roth & Stacey, 1989). Subsequently, symbiosomes divide and gradually enlarge. Bacterial differentiation involves endoreduplication and this is controlled by numerous antimicrobial peptides called nodule-specific cysteine-rich (NCR) peptides (Van de Velde *et al.*, 2010; Vinardell *et al.*, 2013; Alunni & Gourion, 2016). NCRs are defensin-like peptides that are targeted to symbiosomes (Mergaert *et al.*, 2003; Van de Velde *et al.*, 2010). Although the infected cells become massively infected by rhizobia, defence responses are well suppressed. Several host genes have been identified that contribute to this suppression, including *Symbiotic Cysteine-rich Receptor Kinase* (*SymCRK*), *Regulator of Symbiosome Differentiation* (*RSD*), *Defective in Nitrogen Fixation 2* (*DNF2*) and *NODULES WITH ACTIVATED DEFENCE 1* (*NAD1*) (Bourcy *et al.*, 2013; Sinharoy *et al.*, 2013; Berrabah *et al.*, 2014; Wang *et al.*, 2016; Domonkos *et al.*, 2017). Mutations in these genes activate strong defence responses in nodules leading to necrotic cell death and/or premature senescence. Proximal to infection zone is the fixation zone, where rhizobia fully differentiate and start to fix nitrogen. The switch from infection to the distal part of the fixation zone (interzone II/III according to Vasse *et al.*, 1990) occurs rapidly, and is marked by changes in cell morphology as well as gene expression. For example, the rhizobial *nif* genes, encoding components of nitrogenase are induced, amyloplasts accumulate, bacteroids markedly enlarge and become radially aligned (Gavrin *et al.*, 2014).

In older nodules, a senescence zone is formed at the basal part of the nodule, where both host cells and rhizobia are degraded (Van De Velde *et al.*, 2006). A key feature of nodule senescence is the increase in proteolytic activities (Pierre *et al.*, 2014). Cysteine protease genes are highly induced in senescent nodules (Perez Guerra *et al.*, 2010; Pierre *et al.*, 2014). Knockdown of cysteine proteinase genes delays nodule senescence, while their ectopic expression induces premature senescence (Pierre *et al.*, 2014). This underlines a crucial role of cysteine proteases in nodule senescence.

NIN is the first gene of the *NIN-like protein* (*NLPs*) family that was identified (Schauser *et al.*, 2005). Two domains are highly conserved in this gene family: a DNA-binding RWP-RK domain and a Phox and Bem1 (PB1) domain involved in protein–protein interaction (Schauser *et al.*, 2005). A first clue that *NIN* also functions at later nodule developmental stages was gained from two weak *nin* alleles: NF10547 (*nin-16*) and NF0440 (Pislariu *et al.*, 2012; Veerappan *et al.*, 2016). Both mutants form nitrogen fixing deficient (Fix[−]) nodules. Here, we analysed these mutants in detail to uncover the role of *NIN* in later nodule developmental stages.

Materials and Methods

Plant material and growth conditions

Medicago (*Medicago truncatula*) ecotypes Jemalong A17 and R108, and two *nin* mutants (*nin-13* and *nin-16*) were used in

this study. *nin-16* was provided by Rebecca Dickstein (University of North Texas); *nin-13* was obtained from the Noble Research Institute (<https://medicago-mutant.noble.org/mutant/>). *nin-16* were backcrossed with R108, and *nin-13* and *nin-16* were crossed (F1 hybrid) according to Chabaud *et al.* (2006). Seven *nin-13* and *nin-16* hybrid F1 plants were genotyped by PCR (primers listed in Supporting Information Table S1). The obtained PCR fragments were sequenced to confirm *Tnt1* insertion positions. Seed sterilisation, germination and *Agrobacterium* msu440 mediated hairy root transformation was performed according to Limpens *et al.* (2004). Medicago plants were grown in perlite saturated with low nitrate (0.25 mM Ca(NO₃)₂) containing Färhaeus (Fä) medium (Catoira *et al.*, 2000) at 21°C and a 16 h : 8 h, light : dark regime. After 1 wk of growth, plants were inoculated with *Sinorhizobium meliloti* 2011 wild-type or constitutively expressing green fluorescent protein (GFP) or carrying the *PronifH::GFP* reporter (OD₆₀₀ = 0.1, 2 ml per plant).

RNA isolation and qRT-PCR

RNA was isolated from 2-wk-old nodules using the EZNA Plant RNA mini kit (Omega Bio-tek, Norcross, GA, USA). Here, 1 µg RNA was used for cDNA synthesis with the iScript cDNA synthesis kit (Bio-Rad). Real-time qPCR was performed in 10 µl reactions using SYBR Green Supermix (Bio-Rad) and a CFX real-time system (Bio-Rad). Primers are listed in Table S1. Gene expression was normalised using *ACTIN2* as a reference gene.

Constructs

NIN promoter (*ProNIN*_{3C-5kb}) and *ProNIN*_{3C-5kb}:*NIN* construct are described in Liu *et al.* (2019b). To construct *ProNIN*_{3C-5kb}:*GFP-NIN*, *ProNIN*_{3C-5kb}:*NIN-GFP* and *ProNIN*_{3C-5kb}:*NIN*_{ΔPB1}, MultiSite Gateway (Thermo Fisher Scientific, Waltham, MA, USA) was used. pENTR-4,1 and pENTR-1,2 contained the 3C and 5 kb regions of the *NIN* promoter, respectively, pENTR-2,3 was used to introduce coding sequences and 35S terminator (35Ster). *NIN* coding sequence was amplified (full-length *NIN* or truncated *NIN* without the PB1 domain, the 3'-UTR region of *NIN* was not included) by PCR using Medicago A17 nodule cDNA as template, Phusion high-fidelity DNA polymerase (Finnzymes) and specific primers listed in Table S1. To make an N- or C-terminus GFP fusion with *NIN*, pENTR-TOPO-*NIN* together with pENTR-4,1-35S:GFP and pENTR-2,3-35Ster or pENTR-2,3-GFP-35Ster were recombined into Gateway binary vector pKGW-RR-MGW using LR Clonase II plus (Invitrogen) to generate *Pro35S:GFP-NIN-35Ster* or *Pro35S:GFP-NIN-GFP-35Ster*. To fuse *NIN*_{ΔPB1} to 35S terminator, pENTR-TOPO-*NIN*_{ΔPB1} together with pENTR-4,1-35S:GFP and pENTR-2,3-35Ster were recombined into a pKGW-RR-MGW to generate *Pro35S:GFP-NIN*_{ΔPB1}-35Ster. These constructs were used to amplify *GFP-NIN-35Ster/NIN-GFP-35Ster/NIN*_{ΔPB1}-35Ster by PCR using the forward primers with attB2 (GGGGACAGCTTTCTTGACAAAGTGGAA) and reverse primers with attB3 (GGGGACAACCTTTGTATAATAAAGTTGC) (Table S1). By the BP reaction these PCR fragments were introduced into pENTR-2,3. Finally, the MultiSite Gateway

reaction was performed to assemble pENTR-2,3-*GFP-NIN-35Ster*/*NIN-GFP35Ster/NIN_{ΔPBI}-35Ster* with *NIN* promoter regions in pENTR-4,1 and pENTR-1,2 (TOPO) into the Gateway binary vector pKGW-RR-MGW.

Microscopy

Embedding of plant tissue in Technovit 7100 (Heraeus Kulzer), sectioning and staining were performed according to Xiao *et al.*, 2014. Sections were analysed with DM5500B microscope equipped with a DFC425C camera (Leica). Bright-field images were taken under a stereo microscope (M165 FC, Leica). Hand-sectioned nodules were examined using a Leica SP8 confocal microscope, excitation wavelengths of 488 nm and 543 nm were used for GFP/SYTO 9 and propidium iodide/DsRED, respectively. The accumulation of phenolic compounds was visualised by potassium permanganate staining (Bourcy *et al.*, 2013). Live and dead staining of bacteria was performed as described by Haag *et al.* (2011).

Bacterial length measurement

R108 and *nin-13/16* were inoculated with *Sinorhizobium meliloti* 2011 constitutively expressing GFP. At 2 wk after inoculation, photographs of bacteria were taken using a Leica SP8 confocal microscope. The length of bacteria was measured using IMAGEJ software (Schneider *et al.*, 2012).

RNA *in situ* hybridisation

RNA *in situ* hybridisation was conducted using Invitrogen ViewRNA ISH Tissue 1-Plex Assay kits (Thermo Fisher Scientific) according to manufacturer's user guide and optimised for Medicago root and nodules sections (Kulikova *et al.*, 2018). RNA ISH probe sets were designed and synthesised at Thermo Fisher Scientific. Catalogue numbers are VF1-20312 for *NIN* (Medtr5g099060), VP2W7MP for *CP2* (Medtr5g022560), VP7DPDU for *SymCRK* (Medtr3g079850), VPRWEMC for *NAD1* (Medtr7g022640) and VF-20311 for *NF-YA1* (Medtr1g056530). Each probe set was tested on tissue where it should not be present, in this case on noninoculated roots. As a negative control for each hybridisation procedure any probe set was omitted. In both cases no hybridisation signals were detected. The *in situ* images were taken with an AU5500B microscope equipped with a DFC425c camera (Leica).

RNA sequencing analyses

R108 and *nin-16* nodules were harvested 2 wk post inoculation. Three biological replicates were prepared for RNA sequencing (RNA-seq). Total RNAs were isolated using the Qiagen RNeasy mini kit in accordance with the manufacturer's protocol. Isolated RNA samples were quality checked using an Agilent 2100 Bioanalyzer. Subsequently, an RNA-seq library was constructed and sequenced on an BGISEQ-500 platform with paired-end reads at BGI (Hong Kong). About 4 Gb cleaned reads were obtained for

each sample. Sequence reads were mapped to the *M. truncatula* genome v.5.0 (Pecrix *et al.*, 2018) using the CLC genomics workbench 10.0.1 (Qiagen). Length fraction and similarity fraction were set to 0.9 during mapping and only uniquely mapped reads were considered in the analysis. All other parameters were set as default. Transcripts per million (TPM) (Wagner *et al.*, 2012) and differential expression analyses were performed using the CLC genomic workbench 10.0.1. The criteria of fold change ≥ 4 , false discovery rate (FDR) P -value ≤ 0.01 and average TPM ≥ 5 were used to identify the differentially expressed genes.

Results

NIN is highly expressed in the nodule infection zone

According to the *M. truncatula* gene expression atlas, *NIN* is expressed in root nodules (Fig. S1). To determine in which stage of nodule development *NIN* could play a role, we performed RNA *in situ* hybridisation using a *NIN*-specific probe set (Materials and Methods). This showed that in 2-wk-old nodules, *NIN* was expressed highest in the infected cells of the infection zone and the expression level was very low in the non-infected cells (Fig. 1a–c). *NIN* mRNA was also detected in the nodule vasculature (Fig. 1a). In the meristem and distal part of the infection zone the expression of *NIN* was very low (Fig. 1b), whereas in the proximal cell layers of the infection zone, expression of *NIN* was highest (Fig. 1a,b). At the transition from infection to fixation zone *NIN* expression level suddenly dropped (Fig. 1a–c). This switch coincides with amyloplast accumulation at the periphery of the infected cells (Fig. 1c) (Gavrin *et al.*, 2014). A very low level of *NIN* expression was maintained throughout the fixation zone (Fig. 1a–c). The results of RNA *in situ* hybridisation are consistent with laser capture transcriptome data (Table S2) (Roux *et al.*, 2014). This expression pattern suggests that *NIN* plays a role in processes that occur in the infection zone and/or at the transition from infection to fixation zone.

NIN is nuclear located and is present at highest level in the proximal part of the infection zone

Studies on some NLPs have shown that they are located in the cytoplasm under low nitrate conditions and are translocated to the nucleus when the concentration of nitrate is high (Marchive *et al.*, 2013; Cao *et al.*, 2017; Lin *et al.*, 2018). To determine in which cells *NIN* is located in nuclei, where it can induce expression of its target genes, we studied its subcellular localisation in nodules. The functional promoter of *NIN* (Liu *et al.*, 2019b) was used to express *NIN*-tagged with GFP at its C- or N-terminus (*ProNIN_{3C-5kb}:NIN-GFP* or *ProNIN_{3C-5kb}:GFP-NIN*) in the *nin* knockout mutant *nin-1* (Marsh *et al.*, 2007). At 4 wk after inoculation, pink nodules were formed in both cases (Fig. 2a,f), showing that both GFP fusions are biologically functional. Sections of these nodules showed that both C- and N-terminus *NIN-GFP* fusions localised in the nuclei in the meristem, infection zone,

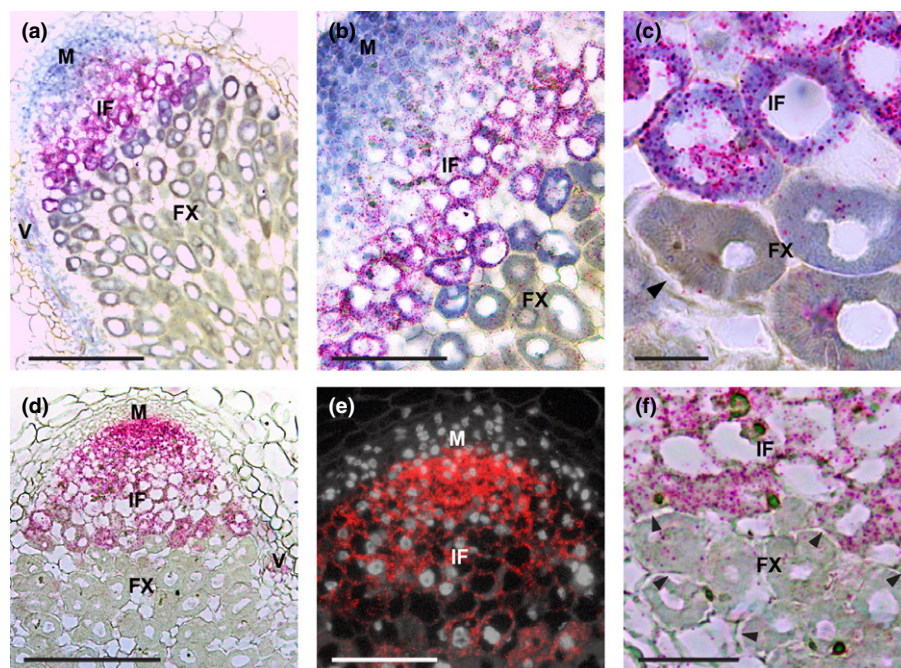


Fig. 1 *NIN* and *NF-YA1* expression pattern in *Medicago* A17 nodule. An overview (a, d) and close-up pictures (b, c, e, f) of RNA *in situ* localisation of *NIN* (a–c) or *NF-YA1* (d–f) in a nodule at 2 wk post inoculation (wpi). Hybridisation signals are visible as red dots. Arrowheads indicate amyloplast deposition. M, meristem; IF, infection zone; FX, fixation zone; V, vasculature. Bars: (a, d) 200 μ m; (b, e) 100 μ m; (c) 20 μ m; (f) 50 μ m.

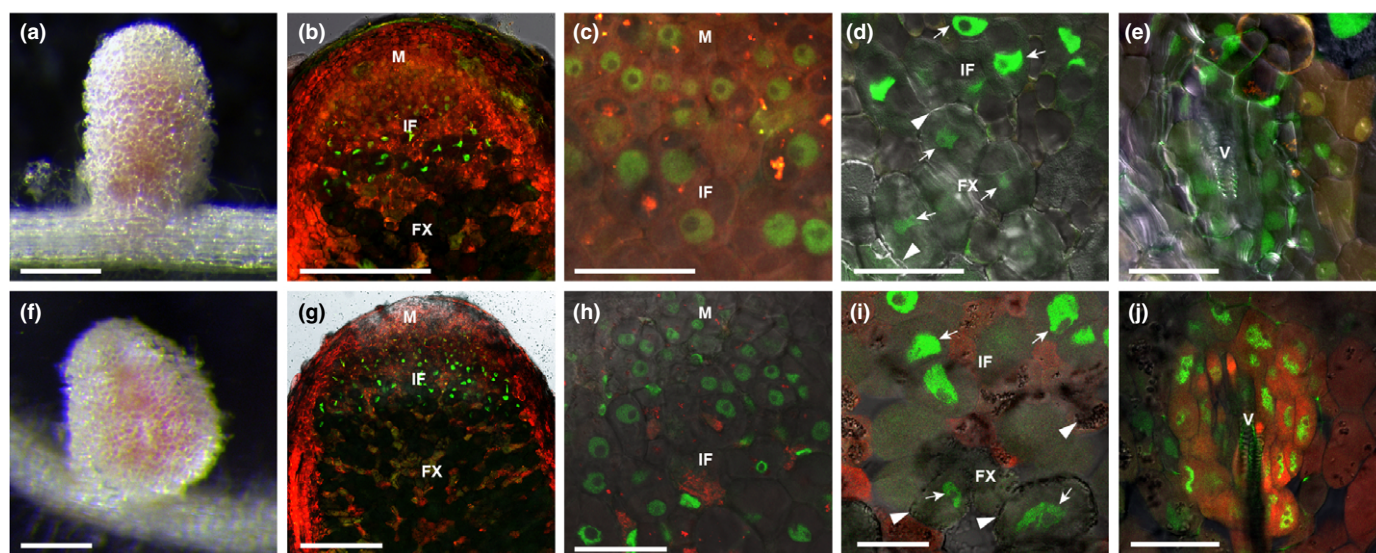


Fig. 2 *NIN* protein is nuclear located in *Medicago* nodules. Pink nodules formed on *nin-1* roots transformed with *ProNIN:NIN-GFP* (a) and *ProNIN:GFP-NIN* (f) constructs at 6 wk post inoculation (wpi). Confocal images show that both *NIN-GFP* (b–e) and *GFP-NIN* (g–j) are located in the nucleus of cells in the meristem (c, h), infection zone (b–d, g–i), fixation zone (d, i) and vasculature (e, j). Transgenic roots were identified by *DsRED* fluorescent (red colour). Arrowheads indicate amyloplast deposition. Arrows indicate nucleus. M, meristem; IF, infection zone; FX, fixation zone; V, vasculature. Bars: (a, f) 2 mm; (b, g) 250 μ m; (c–e, h–j) 40 μ m.

fixation zone and nodule vasculature (Fig. 2b–e,g–j). So, in all cells where *NIN* is expressed, *NIN* is located in the nucleus. *NIN* occurred at a very low levels in the distal part of the infection zone and at markedly higher levels in the proximal cell layers of infection zone (Fig. 2b,g). At the transition to the fixation zone, the *NIN-GFP/GFP-NIN* protein level dropped markedly, similar to the *NIN* mRNA (Fig. 2b,d,g,i).

The expression level of *NF-YA1* does not correlate with the level of *NIN*

NF-YA1 has been shown to be a direct target of *NIN* in *Lotus* (*Lotus japonicus*) (Soyano *et al.*, 2013). To test whether the level of *NIN* correlates with the level of *NF-YA1* expression in *Medicago* nodules, we determined the expression pattern of *NF-YA1*

using RNA *in situ* hybridisation. This showed that *NF-YAI* was expressed in the entire infection zone as found for *NIN* (Fig. 1d). However, differently from *NIN*, the expression level of *NF-YAI* was high in the proximal part but not detectable in the distal part of the meristem (Fig. 1e). *NF-YAI* was also highly expressed in the distal part of infection zone, after which it decreased (Fig. 1d, e). At the transition to the fixation zone, its expression level markedly dropped as for *NIN* (Fig. 1f). Like *NIN*, *NF-YAI* was also expressed in the nodule vasculature (Fig. 1d). So the spatial expression patterns of *NIN* and *NF-YAI* were similar, but the expression level of *NF-YAI* did not correlate with that of *NIN*. This difference indicates the complexity of regulation of *NF-YAI* by *NIN* and suggests that additional transcription factors are involved.

nin-13 and *nin-16* nodules showed premature senescence, defence responses and defects in symbiosome differentiation

To study the function of *NIN* in nodules, we analysed two weak alleles of *nin* (NF10547 and NF0440) that have been reported to form nonfunctional nodules (Pislariu *et al.*, 2012; Veerappan *et al.*, 2016). NF10547 was named *nin-16*, and we named NF0440 *nin-13*. *nin-16* is a monogenic recessive mutant (Veerappan *et al.*, 2016), with a *Tnt1* insertion in the last exon, between the DNA-binding domain (RWP-RK) and protein–protein interaction domain (PB1) (Fig. 3a). *nin-13* also has a *Tnt1* insertion between the RWP-RK and PB1 domains, but in *nin-13* it is located 22 bp upstream of that in *nin-16* (Fig. 3a). At 2 wk after inoculation, *nin-16* had formed white nodules indicating that they were not functional (Fig. 3e). This was confirmed by inoculation with *Sinorhizobium meliloti* 2011 containing *PronifH::GFP*. *PronifH::GFP* was highly expressed in the fixation zone of wild-type nodules, but not in *nin-16* nodules (Fig. 3f,g). The number of nodules formed on *nin-16* was similar to that of wild-type (R108) (Fig. 3b), indicating that nodule initiation was not affected. Semithin sections of *nin-16* nodules showed that an apical meristem was formed (Fig. 3k), infection threads penetrated nodule cells and rhizobia were released and had divided (Fig. 3m). However, before the rhizobia were fully elongated, nodule development was arrested and premature senescence was induced (Fig. 3o). This was also supported by live/dead staining of rhizobia that showed many dead bacteria in infected cells (Fig. S2). *nin-13* displayed the same nodule phenotype as *nin-16* (Fig. S3). F1 plants obtained by crossing these two mutants also had the same nodule phenotype, confirming that these mutants were allelic (Fig. S4). In the subsequent studies we mainly focused on *nin-16*.

To determine when rhizobial development was blocked in the *nin-16* mutant nodules, we measured the length of the rhizobia (Fig. 3c). In both wild-type and mutant nodules the rhizobia in the infection thread, or just released from it, were about 1 μm long. In the most proximal part of infection zone of the wild-type nodules, the symbiosomes were about 3.5 μm in length. After the transition to the fixation zone, the fully differentiated rhizobia were about 8 μm long. Rhizobia in *nin-13/16* nodules could

reach a length of *c.* 3.5 μm (Fig. 3c). This in combination with the lack of *nif* expression, indicated that the block of differentiation occurred at the stage when, in the wild-type, the transition from infection to fixation zone takes place.

The block in rhizobia differentiation might be due to premature senescence and a not sufficiently suppressed defence response. The accumulation of phenolic compounds is commonly used to identify a defence response in nodules (Bourcy *et al.*, 2013; Berrabah *et al.*, 2015, 2018; Wang *et al.*, 2016; Domonkos *et al.*, 2017). Potassium permanganate/methylene blue staining showed that phenolic compounds indeed accumulated in *nin-16* nodules (Fig. 3i). This means that a defence response was induced in mutant nodules.

PB1 domain of *NIN* is not essential for nodule development

The *Tnt1* insertion in both *nin-13* and *nin-16* will result in a truncated *NIN* protein lacking the protein–protein interaction domain (PB1). To test whether the *nin-13/16* phenotype is caused by the absence of the PB1 domain, we introduced a construct encoding a truncated *NIN* (deletion starts at the position of the *Tnt1* insertion in *nin-16*, including the PB1 domain) (*ProNIN*_{3C-5kb::NIN Δ PB1}) into the knockout mutant *nin-1* by hairy root transformation. Surprisingly, pink nodules were formed on transgenic roots 4 wk after inoculation (Fig. 4a). Next, we inoculated transgenic roots with rhizobia containing *PronifH::GFP*, and *nifH* was highly induced in the formed nodules (Fig. 4c,d). Semithin sections of these nodules revealed that 23 out of 67 (34.3%) were wild-type-like (Fig. 4b), comparable with 12 out of 38 (31.6%) wild-type-like nodules formed on *nin-1* roots transformed with full-length *NIN* (*ProNIN*_{3C-5kb::NIN}). This suggests that the PB1 domain of *NIN* is not essential for the formation of functional nodules.

Reduced *NIN* mRNA level in the cytoplasm of *nin-13/16* nodule cells

The transition from infection to fixation zone does not occur in *nin-13/16*. As *NIN* accumulates at a high level at this transition site, we analysed the *NIN* expression pattern in *nin-13/16* nodules by RNA *in situ* hybridisation. As found in wild-type (R108) nodules (Fig. 5a), *NIN* was highly expressed in the infection zone of the mutant nodules (Fig. 5b,c), however there was a marked difference between *nin-13/16* and wild-type nodules. *NIN* RNA in *nin-13/16* nodules accumulated to higher levels in nuclei compared with in the cytoplasm, which is not the case in wild-type nodules (Fig. 5d,e,f). This indicated that the transport of *NIN* mRNA from the nucleus to the cytoplasm was hampered. By contrast, transport of *NF-YAI* RNA was not affected (Fig. S5), suggesting that the inhibition of mRNA transport was most likely to be specific for *NIN* in *nin-13/16*. By quantitative real-time PCR (qRT-PCR) we showed that *NIN-Tnt1* fusion transcripts were formed in *nin-13/16* nodules (Fig. S6). In *nin-13*, about 80% of *NIN* transcripts contained *Tnt1* sequences, and about 60% of *NIN* transcripts contained *Tnt1* sequences in *nin-16* (Fig. S6). Moreover, *nin-16* RNA sequencing data (see below)

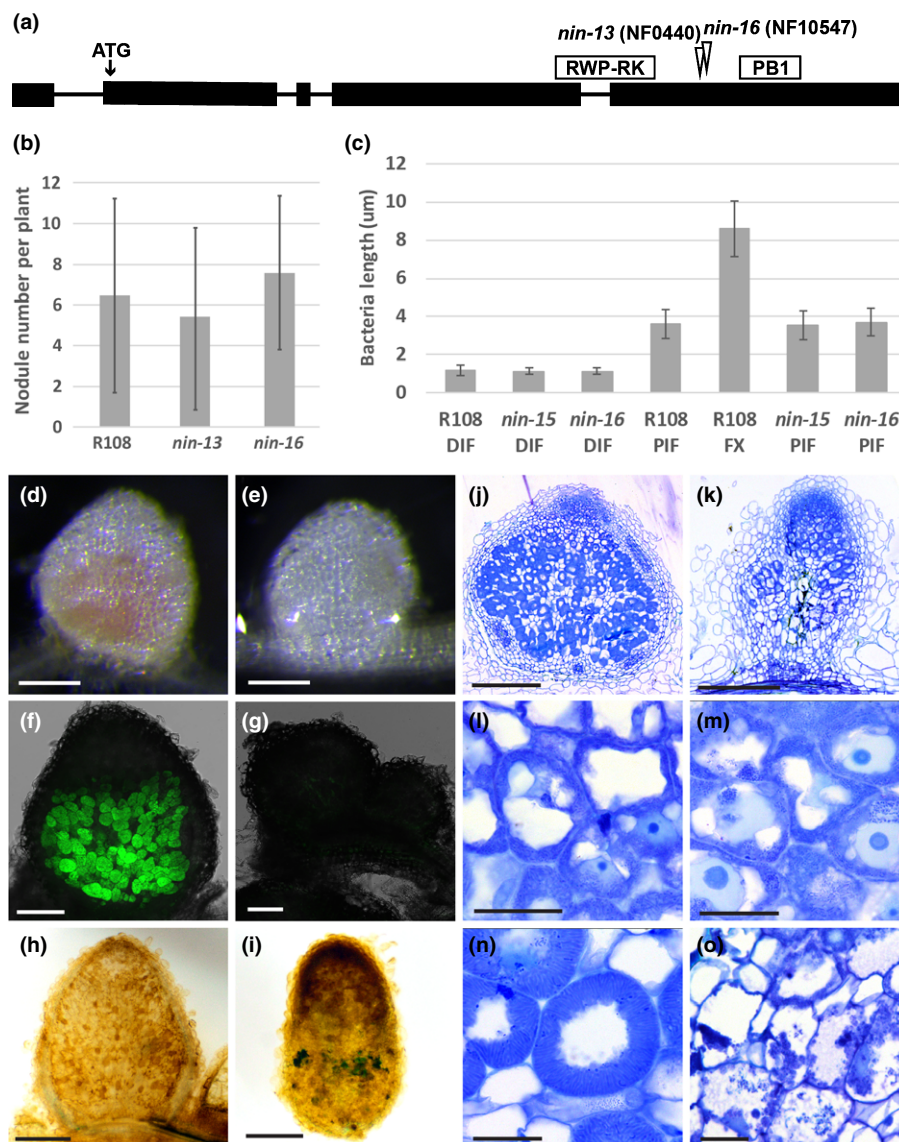


Fig. 3 Phenotype of *Medicago* *nin-13* and *nin-16* mutants. (a) Schematic representation of the *Tnt1* insertion site in *nin-13* and *nin-16* alleles. Exons of *NIN* are shown as black boxes, and introns are represented by lines. (b) The number of nodules formed on R108 (wild-type), *nin-13* and *nin-16* are similar. Nodule numbers per plant ($n = 19$) were counted at 2 wk post inoculation (wpi). Data are means \pm SD. (c) Rhizobia in *nin-13/16* were able to elongate to the size that in wild-type plants reached before the transition to the fixation zone. Bacteria length are measured at 2 wpi. $n \geq 70$, data are means \pm SD. DIF, distal part of infection zone; PIF, proximal part of infection zone; FX, fixation zone. At 2 wpi with *Sinorhizobium meliloti* 2011, wild-type nodules were pink (d) whereas *nin-16* nodules remained white (e) that indicate the absence of leghaemoglobin. Formation of nonfunctional nodules on *nin-16* was further confirmed by inoculation with *Sinorhizobium meliloti* 2011 carrying the *PronifH::GFP* reporter construct (f, g). *nifH* was highly induced in R108 (f) but not induced in *nin-16* nodules (g). Semithin sections stained with toluidine blue show that in comparison with wild-type nodules (j, l, n), an apical meristem was formed on *nin-16* mutant nodule (k), rhizobia were released and divided (m), however, their development was arrested, and premature senescence was induced (o). Potassium permanganate/methylene blue staining shows accumulation of phenolic compound in *nin-16* nodule (i), but not in wild-type nodule (h). *nin-13* shows similar phenotype as *nin-16*, figures shown in Supporting Information Fig. S3. Bars: (d, e) 2 mm; (f, g) 200 μ m; (h, i) 500 μ m; (j, k) 300 μ m; (l–o) 30 μ m.

revealed that some reads were mapped to the intron and promoter region of *NIN* (Fig. S7). The frequency of aberrantly spliced *NIN* transcripts in *nin-16* was between 30.24% and 64.80%. This is markedly higher than in R108, in which this frequency was between 1.39% and 4.37% (Fig. S7). This finding indicated that the *Tnt1* insertion affected *NIN* transcription and splicing. As the export of unspliced and incompletely spliced transcripts from nuclei is prevented (Schmid & Jensen, 2008),

we assumed that this might have caused the reduced transport of *NIN* RNA to the cytoplasm. By using *NIN*-specific primers (upstream of *Tnt1* insertion), we showed that the expression level of *NIN* in wild-type and mutant nodules was similar (Fig. 5g,h). As a substantial part of *NIN* mRNA had accumulated in nuclei of *nin-13/16*, the level of *NIN* mRNA that can be translated (in the cytoplasm) was reduced, this might have caused the phenotype of *nin-13/16* nodules.

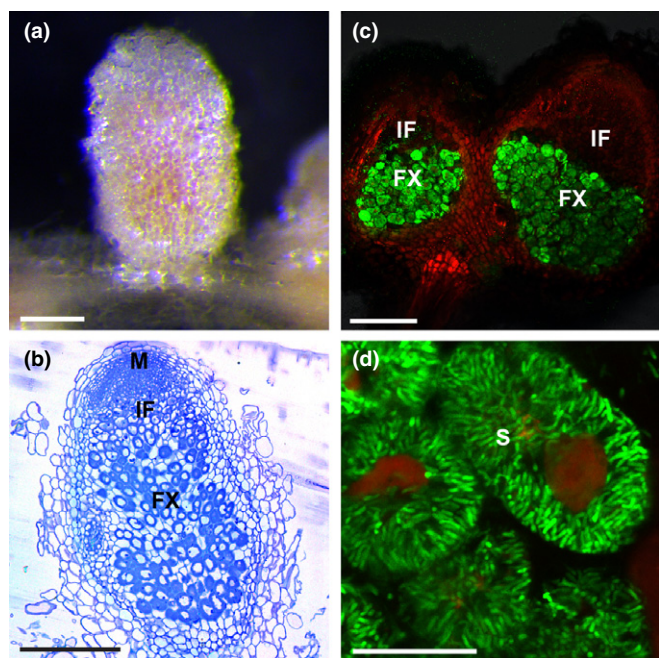


Fig. 4 Wild-type-like pink nodules formed on *Medicago nin* knock-out mutant (*nin-1*) roots transformed with truncated *NIN* $_{\Delta PB1}$. Pink nodules formed on *nin-1* roots transformed with *ProNIN* $_{3C-5kb}$:*NIN* $_{\Delta PB1}$ at 4 wk post inoculation (wpi) (a). Semithin sections of the nodules stained with toluidine blue display normal zonation (b). Confocal image of nodules formed on the *ProNIN* $_{3C-5kb}$:*NIN* $_{\Delta PB1}$ transgenic *nin-1* roots at 4 wpi with a rhizobial strain carrying *nifH::GFP* showed that *nifH* is highly expressed in the fixation zone (c). Close-up of nodule cells in fixation zone, showing well developed symbiosomes (d). M, meristem; IF, infection zone; FX, fixation zone; S, symbiosome. Bars: (a) 2 mm; (b) 300 μ m; (c) 250 μ m; (d) 30 μ m.

To test this hypothesis, we introduced *ProNIN* $_{3C-5kb}$:*NIN* $_{\Delta PB1}$ into *nin-16* by hairy root transformation. Semithin sections of the nodules formed on transgenic roots showed that symbiosome development was restored (symbiosomes reached the length about 8 μ m) and the defence/premature senescence phenotype was markedly reduced (Fig. S8). This result supports the conclusion that the *nin-13/16* nodule phenotype is caused by a reduced *NIN* mRNA level, but not the absence of the PB1 domain of *NIN*.

nin-16 nodule transcriptome switched from symbiosis to defence/senescence-related processes

To determine which *NIN*-controlled processes were disturbed in *nin-13/16* mutants, we compared the transcriptomes of 2-wk-old *nin-16* and wild-type nodules; 31 841 gene transcripts were detected in these nodules (Table S2). We identified 2744 genes that were differentially expressed in *nin-16* nodules compared with wild-type (Table S3) of which 1281 (46.7%) genes were upregulated and 1463 (53.3%) genes were downregulated in *nin-16* (Table S3).

The histology of the *nin-13/16* nodules indicated that the infection zone was not much affected, whereas a fixation zone was not formed. Consistent with this finding is that only a small fraction of the genes that are especially expressed in the meristem

or the distal part of the infection zone of wild-type nodule (according to Roux *et al.*, 2014) is differentially expressed in *nin-16*. By contrast, a markedly higher percentage of genes that are especially expressed in fixation zone of wild-type nodules is differentially expressed (Table 1). However, for the genes especially expressed in the proximal part of the infection zone of wild-type nodules, the percentage of differentially expressed genes in *nin-16* was also high (Table 1). The few differentially expressed genes that are especially expressed in the distal part of the infection zone were mainly upregulated (Table 1). Several of these upregulated genes are related to the defence response (Table S4). By contrast, differentially expressed genes that are especially expressed in the proximal part of the infection zone or the distal part of the fixation zone (interzone II/III according to (Roux *et al.*, 2014)) in wild-type nodules, were mainly downregulated (Table 1). Most of these genes were related to symbiotic functions such as *leghaemoglobin* and *NCR* genes (Table S4). For the genes especially expressed in the proximal part of the fixation zone (zone III, according to Roux *et al.*, 2014), for which the expression level was changed, similar numbers were upregulated and downregulated, respectively (Table 1). The upregulated genes were mainly related to senescence and defence and downregulated genes included symbiotic genes (Table S4). We do not know in which part of the *nin-13/16* nodules the upregulated genes are expressed and this could be different from their expression in wild-type nodules. For example, the defence-related genes that are expressed in the meristem of wild-type nodules might be induced in the early senescence zone of *nin-13/16* nodules.

Consistent with the fact that the early nodule developmental stages were not much affected, the expression levels of genes required for intracellular infection were not significantly changed. This group included *Ethylene response factor* (*ERF*), transcription factor *required for nodulation 1* (*ERN1*) and direct targets of *NIN*, *NF-YA1* and *nodulation pectate lyase* (*NPL*) (Fig. 6b) (Xie *et al.*, 2012; Soyano *et al.*, 2013; Laporte *et al.*, 2014). Release of rhizobia from infection threads occurred in the distal part of the infection zone. The symbiotic exocytosis pathway-related genes *Vamp721d*, *Vamp721e* and *SYPI3II* are important for release (Ivanov *et al.*, 2012; Huisman *et al.*, 2016). Their level of expression in *nin-16* nodules was not significantly changed (Fig. 6b), which was consistent with the occurrence of release.

In *nin-16* nodules, rhizobia elongated and reached a size that in wild-type nodules is characteristic for rhizobia in the most proximal part of the infection zone (Fig. 3c). The elongation of rhizobia was initiated in *nin-16* nodules (Fig. 3c) and this was consistent with an unaffected or even upregulated expression level of some *NCR* genes that were expressed in the infection zone (Fig. 6a; Table S2). The block in further differentiation might be caused by the lack of fixation zone formation, where other *NCR* genes are expressed. The accumulation of phenolic compounds and the induction of premature senescence suggested that defence/senescence was not sufficiently suppressed in *nin-13/16* nodules. Consistent with this, there were many defence/senescence-related genes that were significantly upregulated in *nin-16* nodules (Fig. 6a; Table S5) including well known marker genes such as *PR10* (16.9-fold upregulated) and *NDR1* (8.7-fold

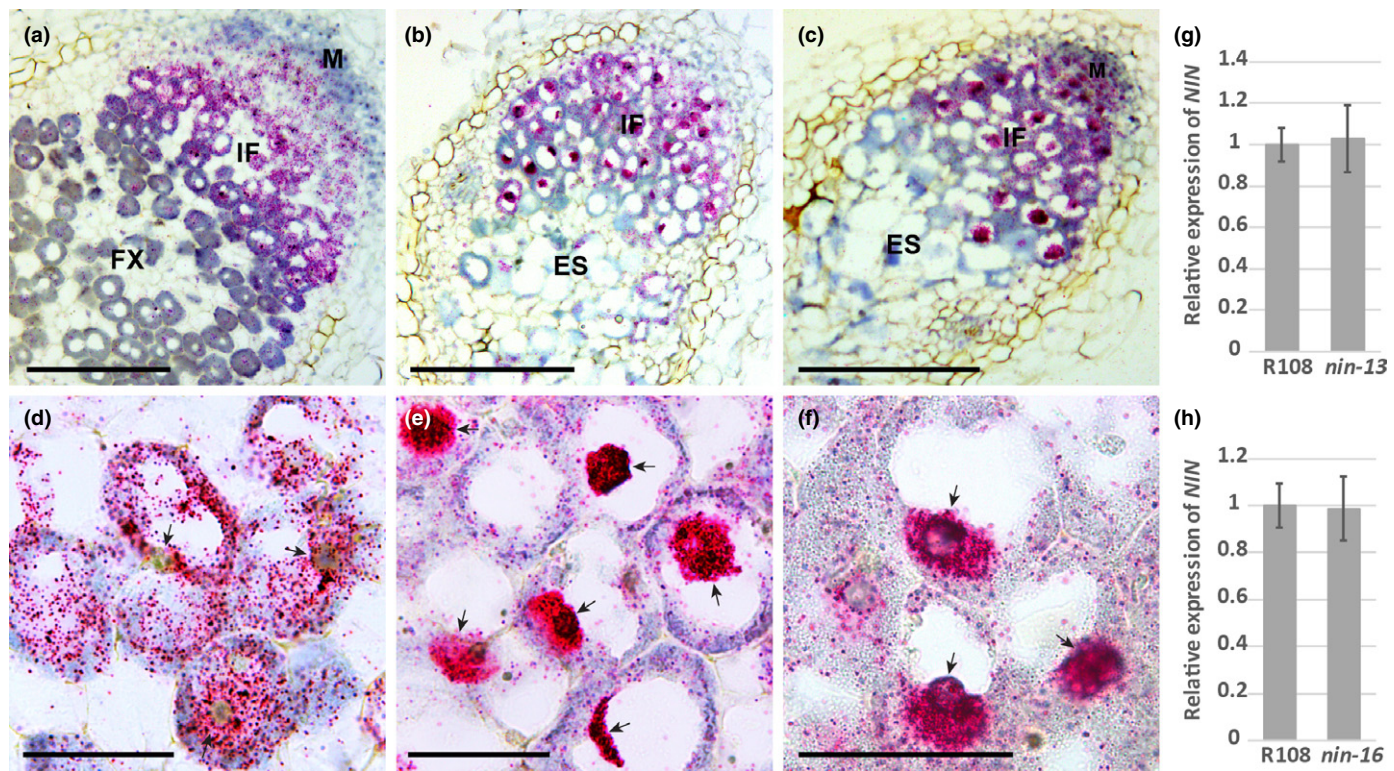


Fig. 5 *NIN* mRNA level reduced in the cytoplasm of nodule cells of *Medicago nin-16*. RNA *in situ* localisation of *NIN* shows that the substantial part of *NIN* mRNA accumulates in nuclei of *nin-13* (b, e) and *nin-16* nodule cells (c, f), compared with wild-type (R108) nodule section (a, d). Hybridisation signals are visible as red dots (a–f). Arrows indicate the nuclei (d–f). M, meristem; IF, infection zone; FX, fixation zone; ES, early senescence zone. Quantitative reverse transcription polymerase chain reaction (qRT-PCR) shows that *NIN* expression level in wild-type (R108), *nin-13* and *nin-16* nodules were similar (g, h). Data are means \pm SD of three biological replicates. Bars: (a–c) 250 μ m; (d–f) 40 μ m.

Table 1 Analysis of genes specifically expressed in different *Medicago* wild-type nodule developmental zones (Roux *et al.*, 2014) differentially expressed in *nin-16*.

Genes 70% expressed in zone:	Meristem	Distal infection zone	Proximal infection zone	Distal fixation zone (interzone)	Proximal fixation zone (zone III)
Total number of genes	1901	370	191	665	536
Number of genes differentially expressed in <i>nin-16</i>	126	24	51	184	82
Percentage of genes of differentially expressed in <i>nin-16</i>	6.63%	6.49%	26.70%	27.67%	15.30%
Number of genes up regulated in <i>nin-16</i>	101	21	1	2	35
Percentage of genes up regulated in <i>nin-16</i>	80.16%	87.50%	1.96%	1.09%	42.68%
Number of genes down regulated in <i>nin-16</i>	25	3	50	182	47
Percentage of genes down regulated in <i>nin-16</i>	19.84%	12.50%	98.04%	98.91%	57.32%

Darker shade indicates higher percentage of genes differentially expressed in *nin-16*. Higher percentage of genes up regulated in *nin-16* shown in darker red colour; higher percentage of genes downregulated in *nin-16* shown in darker green colour.

upregulated) (Fig. 6b; Table S3). The expression of flavonoid biosynthesis genes also supported the occurrence of a defence response. Among 38 differentially expressed genes, 28 were upregulated. Most of these genes had putative chalcone synthase activity or chalcone isomerase activity that is involved in the formation of flavonoid scaffolds. By contrast, all the 10 downregulated genes had putative glucosyltransferase activity that was related to the diversity of flavonoids (Fig. 6a; Table S5) (Saito *et al.*, 2013). Cysteine proteases (CPs) and vacuolar processing

enzyme (VPE) have been shown to play a crucial role in the onset of nodule senescence and their expression can also be the consequence of plant defence responses (Sheokand & Brewin, 2003; Grudkowska & Zagdańska, 2004; Hara-Nishimura *et al.*, 2005; Wang *et al.*, 2016). In *nin-16* nodules, CP2 and VPE are 202.6-fold and 13.6-fold upregulated, respectively (Fig. 6b; Table S3), and they were among the most highly expressed genes (Table S2). Moreover, genes involved in suppression of plant defence in nodules such as *DNF2*, *SymCRK*, *NAD1* and *RSD* were 1.6–,

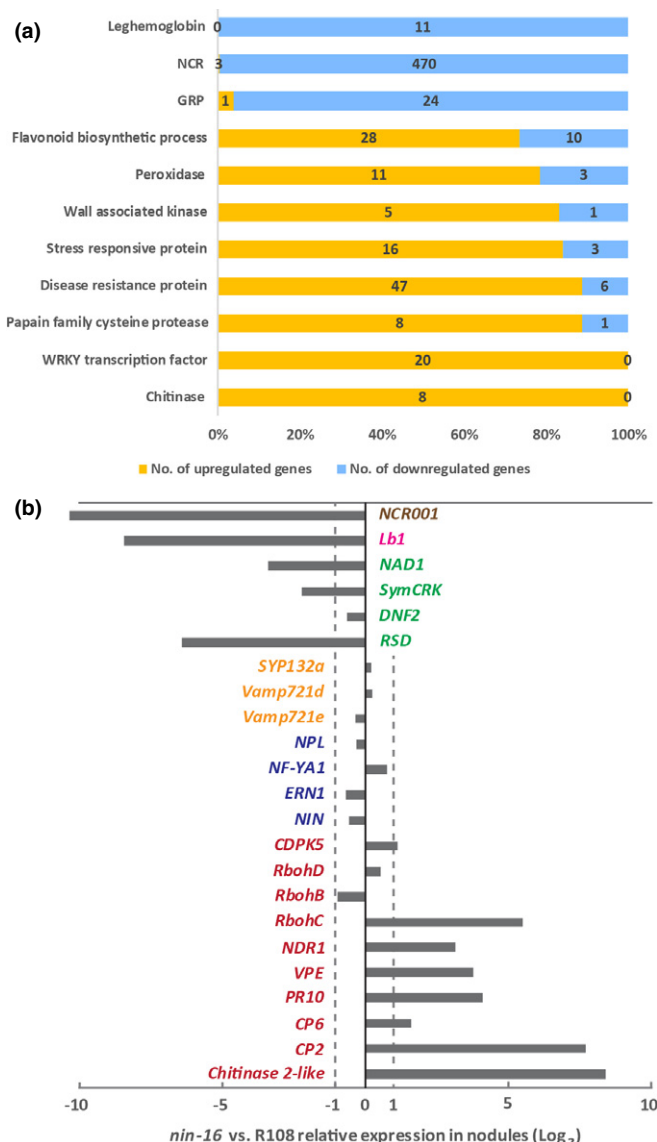


Fig. 6 Medicago *nin-16* transcriptome is consistent with the reduced suppression of defence and early senescence. Transcriptional regulation of gene families/metabolism pathways in nodules (a). The classification of each gene in the families/metabolism pathways is based on the protein function indicated in the Mt 5.0 annotation or gene ontology terms. NCR, Nodule Cysteine-Rich peptide; GRP, Nodule-specific Glycine Rich Peptide. Analysis of representative genes from the transcriptome data (b). Genes required for primordium initiation and infection formation (blue colour), including *NIN* (Nodule inception) itself, *Ethylene response factor required for nodulation 1* (*ERN1*), *Nuclear transcription factor Y subunit A-1* (*NF-YA1*) and *nodulation pectate lyase* (*NPL*). The symbiotic exocytosis pathway-related genes (yellow colour) required for rhizobial release, including *VAMP721d* and *VAMP721e* that are members of the vesicle-associated membrane protein 721 family, and *SYNTAXIN OF PLANTS 132* (*SYN132*). Nodule-specific cysteine-rich (*NCR*) peptides (brown colour) and *leghaemoglobin* (*LB*) (pink colour), are known to be required for bacteria differentiation and nitrogen fixation. Genes related to defence and senescence (red colour), including *calcium-dependent protein kinase* (*CDPK*), *respiratory burst oxidase homologs* (*Rboh*), *cysteine proteinases* (*CPs*), *nonrace-specific disease resistance 1* (*NDR1*), *vacuolar processing enzyme* (*VPE*), *pathogenesis-related protein 10* (*PR10*) and *Chitinase* genes. See detailed information about selected genes in Supporting Information Table S1.

4.7-, 10.6- and 83.9-fold downregulated in *nin-16* (Fig. 6b; Table S2). Taken together, these data supported the conclusion that *nin-16* transcriptome switched from symbiosis to defence/senescence-related processes.

Defence/senescence is suppressed in the infection zone of *nin-13/16* nodules

Many plant defence/senescence-related genes were highly induced in *nin-16* nodules. To determine whether the induction of these genes had already occurred in the infection zone, we used *CP2* as a marker gene as it was the highest expressed defence/senescence-related gene in *nin-16*. *In situ* hybridisation showed that, in 2-wk-old mutant nodules, *CP2* was extremely highly expressed in the infected cells of the premature senescence zone, but not in the infection zone or other nodule tissue (Fig. 7b,c). This suggested that the defence and early senescence response was well suppressed in the nodule infection zone, but that suppression was not sufficient at the stage when transition to fixation zone would occur.

symcrk and *nad1* mutants form nodules in which defence responses are induced and symbiosome differentiation becomes arrested (Berrabah *et al.*, 2014b; Wang *et al.*, 2016; Domonkos *et al.*, 2017; Yu *et al.*, 2018). This is similar to the nodule phenotype of *nin-13/16*. *rsd* and *dnf2* mutants also have a similar nodule phenotype (Bourcy *et al.*, 2013; Sinharoy *et al.*, 2013), however the expression level of *RSD* was very low and the *DNF2* expression level in *nin-16* was not significantly changed (Table S2). To determine when plant defence suppressing genes were activated during nodule development, we checked the expression pattern of *SymCRK* and *NAD1*. RNA *in situ* hybridisation showed that both *SymCRK* and *NAD1* were expressed in the infected cells of the infection zone and that their expression levels increased from the distal to the proximal part (Fig. 7e–h) and was similar to the *NIN* expression pattern (Figs 1a, 5a). However, *SymCRK* and *NAD1* remained expressed at a relatively high level in the fixation zone (Fig. 7e–h), whereas *NIN* expression markedly dropped at the transition from infection to fixation zone (Figs 1a–c, 5a). To determine where in the nodule the expression of defence suppressing genes was affected, we studied *SymCRK* expression in *nin-16* nodules. RNA *in situ* hybridisation showed that *SymCRK* was expressed in the infection zone (Fig. 7d). In the senescing cells, *SymCRK* mRNA was hardly detectable.

These results indicated that the expression level of defence suppressing genes in the infection zone was sufficient to suppress the defence response and early senescence, whereas at the transition to fixation zone, the suppression was no longer sufficient.

Discussion

Here we showed that *NIN* plays, in addition to its previously identified role in infection and nodule organogenesis, a key role in the late steps of nodule development leading to a functional symbiosis. *nin-13/16* nodules displayed a particularly normal infection zone, whereas a fixation zone was not formed. Instead, a

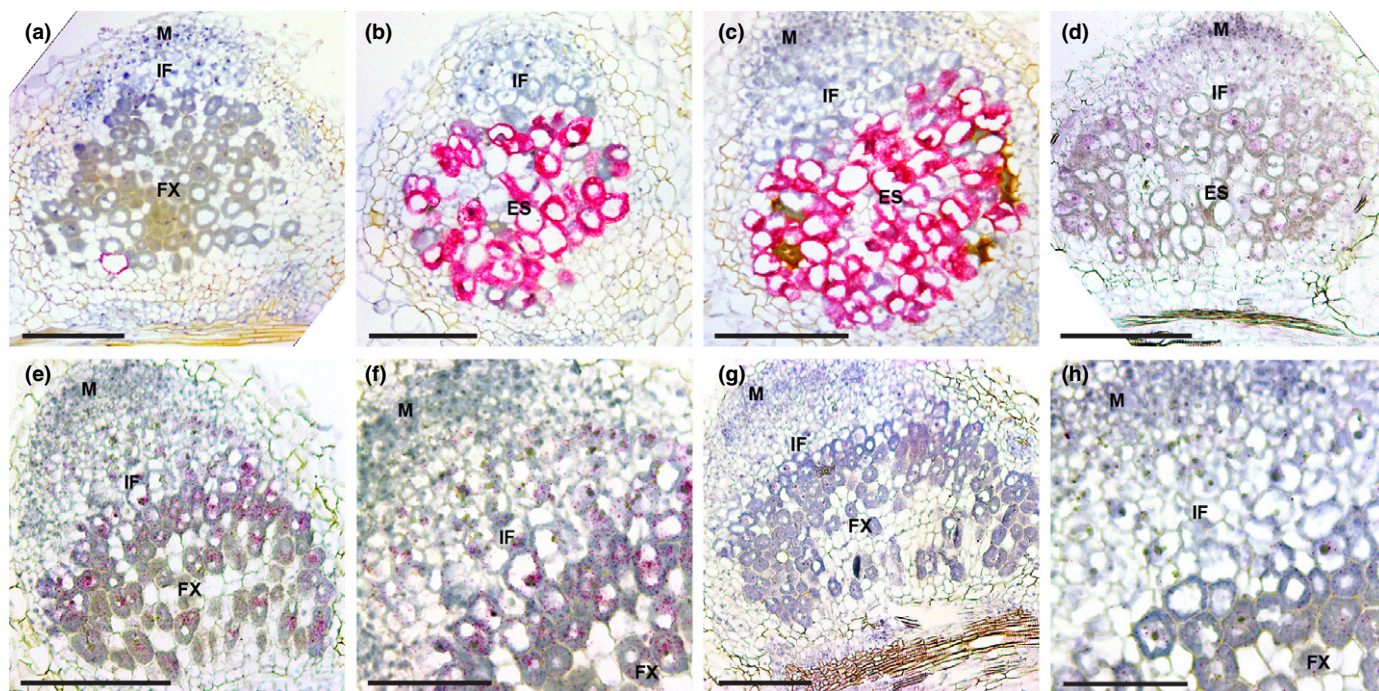


Fig. 7 Expression pattern of defence/senescence response and suppression genes. RNA *in situ* localisation of defence/senescence response gene *CP2* in Medicago R108 (a), *nin-13* (b) and *nin-16* (c) nodules at 2 wk post inoculation (wpi). Overview (e, g) and close-up (f, h) pictures of expression patterns of defence suppression genes *SymCRK* (e, f) and *NAD1* (g, h) in 2 wpi R108 nodules. (d) Expression pattern of *SymCRK* in 2 wpi *nin-16* nodule. Hybridisation signals are visible as red dots. M, meristem; IF, infection zone; FX, fixation zone; ES, early senescence zone. Bars: (a–e, g) 200 μ m; (f, h) 100 μ m.

zone with defence responses and premature senescence occurred. The phenotype is most likely to be caused by reduced *NIN* mRNA levels in the cytoplasm. Consistent with this phenotype, transcriptome analyses of *nin-16* nodules showed that defence/senescence-related genes were highly induced and defence suppressing genes were reduced. However, although defence/senescence seemed well suppressed in the infection zone, the transcriptome is most likely already markedly changed in the proximal part of the nodule infection zone. *NIN* mRNA and protein accumulated at the highest level in the proximal part of the infection zone. At the transition to fixation zone, this level suddenly dropped to a much lower level, suggesting that *NIN* is involved in the switch from infection to fixation zone.

In both *nin-13* and *nin-16*, *Tnt1* is inserted upstream of the region that encodes the PB1 domain, which is located at the carboxy-terminus of *NIN*. Therefore, we expected that loss of this domain would have caused the mutant nodule phenotype. However, by introducing truncated *NIN Δ PB1* into a *nin* knockout mutant (*nin-1*), we showed that the PB1 domain was not necessary for the formation of wild-type-like nodules in Medicago A17 (Fig. 4). The importance of the PB1 domain is underlined by being conserved in the NLP family, including *NIN*. The PB1 domain has been shown to be essential for the formation of homodimers and heterodimers of Arabidopsis NLP6 and NLP7 (Guan *et al.*, 2017). In addition, Medicago NLP1 is required for suppression of nodulation by nitrate, and this suppression probably involves a physical interaction of *NIN* and NLP1 by their PB1 domains (Lin *et al.*, 2018). Therefore, the PB1 domain of *NIN* may be involved in regulating its activity in response to, for

example, exogenous nitrate, whereas it is not essential for intrinsic nodule development.

The *nin-13/16* nodule phenotype is probably caused by reduced *NIN* mRNA levels in the cytoplasm. *In situ* hybridisation showed that a substantial part of *NIN* RNA accumulated in *nin-13/16* nuclei. Furthermore, by introducing truncated *NIN* into *nin-16*, symbiosome development was restored and the defence and early senescence phenotype was markedly reduced. This confirmed that the mutant nodule phenotype was caused by reduced *NIN* mRNA level, but not the absence of the PB1 domain of *NIN*. The *NIN* RNA transcribed from the *nin-16* allele was altered by the *Tnt1* insertion, therefore, it might be possible that this improper nature of the *NIN* transcripts caused (partial) retainment of it in nuclei. Nuclear retention of transcripts might also occur in other mutants with the *Tnt1* insertion. Although the qPCR data showed that *NIN-Tnt1* chimeric sequences were present, they did not prove that full-length *NIN-Tnt1* chimeric sequences were formed, as promoter and terminator regions existed in the identical 5' and 3' long terminal repeats (LTR) of *Tnt1* (Grandbastien *et al.*, 1989; Grandbastien, 2015). It has been shown that some LTR regulatory regions can induce transcription in an opposite direction (Grandbastien *et al.*, 1989; Grandbastien, 2015). This could explain the reads mapped to the promoter region of *NIN* in *nin-16* as a readout transcript of LTR.

In Pislariu *et al.* (2012), more mutants with a *Tnt1* insertion in *NIN* were described. However, except in *nin-13* (NF0440), they all showed a Nod[−] phenotype, including two mutants (NF0825 and NF2700) that had the *Tnt1* insertion at a position that was

downstream of that in *nin-13/16*. However, it cannot yet be concluded that the truncated NIN proteins that are slightly longer than in *nin-13* and *nin-16* are not functional. In both *nin-13* and *nin-16*, *NIN* mRNA is retained in the nucleus. It seems probable that the *Tnt1* insertions in NF0825 and NF2700 also cause such *NIN* mRNA retention. If this is stronger than in *nin-13/16*, this could explain the Nod[−] phenotype of these mutants. It is also possible that other *Tnt1* insertions in these mutants caused the Nod[−] phenotype, as whether the nodule phenotype co-segregates with *Tnt1* insertion in *NIN* has not yet been studied.

Several NLPs are located in the cytoplasm under low nitrate conditions and are translocated to the nucleus under high nitrate conditions (Marchive *et al.*, 2013; Cao *et al.*, 2017; Lin *et al.*, 2018). Here we showed that NIN was located in nuclei in all nodule cells where it is expressed. For the nitrate-triggered translocation to nuclei Ser205 of AtNLP7 becomes phosphorylated. This serine is conserved in several NLPs, but is lacking in NIN (Liu *et al.*, 2017), so NIN might have lost the information required for retention in the cytoplasm.

In *Medicago*, *NIN* is expressed in the infection zone and meristem. This is consistent with findings of a previous study on pea (*Pisum sativum*) (Borisov *et al.*, 2003). Both *NIN* mRNA and NIN protein had reached their highest level in the proximal part of the infection zone in *Medicago* nodules, and this suddenly dropped at the transition to fixation zone. However, it is not clear whether in pea the decrease in *NIN* expression also occurred at the switch to interzone/distal fixation zone or somewhat later (Borisov *et al.*, 2003). The sudden change in the *NIN* levels at transition from the infection to fixation zone coincided with several other rapid changes such as the accumulation of starch, the induction of bacterial *nif* genes and the radial alignment of the symbiosomes (Gavrin *et al.*, 2014). Rapid changes in protein/mRNA activity/levels often involve negative and positive feedback mechanisms. For example, in the Arabidopsis stem cell niche, an asymmetric cell division initiates the formation of root endodermis and cortex. This involves the SHORT ROOT (SHR)/SCARECROW (SCR) complex. This complex induces the expression of *cyclinD6,1* that inactivates RETINOBLASTOMA-RELATED, the repressor of SCR activity. Through this positive feedback loop, the SHR–SCR complex activity increases and triggers asymmetrical division. This was followed by a negative feedback involving degradation of the SHR–SCR complex (Cruz-Ramírez *et al.*, 2012), therefore the accumulation of NIN to a high level, which is followed by a sudden drop, was consistent with a role in a molecular switch. Whether and how NIN is involved in a molecular circuit controlling the switch from infection to fixation zone remains to be studied.

In previous studies on *nin-13/16* (Pislariu *et al.*, 2012; Veerappan *et al.*, 2016), the accumulation of phenolic compounds was not described. The level of accumulation of phenolic compounds in these two mutants seems lower in comparison with some other mutants (Bourcy *et al.*, 2013; Berrabah *et al.*, 2014b; Wang *et al.*, 2016; Domonkos *et al.*, 2017), therefore, it might have been overlooked in previous studies. Furthermore, it has been shown that in some mutants, for example *dnf2* (Berrabah *et al.*, 2014a),

the accumulation of phenolic compounds is conditional. Therefore, it cannot be excluded that less phenolic compounds had accumulated in *nin-13/16* nodules due to different growth conditions. *nin-13* previously has been reported as Nod[−] at 21 d post inoculation with rhizobia (Pislariu *et al.*, 2012). The reason for this difference is not clear, as in all our experiments the nodule number formed on the mutant was similar to that of the wild-type (R108).

Although *nin-13/16* has been reported previously, the phenotypic characterisation was not detailed (Pislariu *et al.*, 2012; Veerappan *et al.*, 2016). Here we analysed the *nin-13/16* nodule phenotype explicitly. Both mutant nodules made an infection zone that at the cytological level was rather normal. Rhizobia were released from infection threads, they multiplied and the symbiosomes started to elongate, reaching the size that is obtained in the proximal part of the infection zone in WT nodules. By contrast, processes that occurred at the transition to fixation zone did not take place. For example, *nif* genes were not induced, symbiosomes did not further elongate and amyloplasts did not accumulate at the periphery of the infected cells. This phenotype is in part consistent with the transcriptome data. Genes that were especially expressed in the fixation zone were downregulated (except genes related to senescence and the defence response). By contrast, expression levels of genes especially active in the distal infection zone were in most cases not affected, except defence-related genes, which were upregulated. It is not known where these upregulated genes are expressed in the *nin-16* nodules. Furthermore, the expression levels of many genes that were especially expressed in the proximal part of the infection zone were already affected, the genes related to symbiotic functions were downregulated.

Symbiosome development became arrested in *nin-13/16* nodules and defence and early senescence were induced. The defence suppressing genes *SymCRK* and *NAD1* were markedly downregulated in *nin-16* nodules. Loss-of-function mutations in these genes caused a similar symbiosome phenotype as found for *nin-16* (Berrabah *et al.*, 2014b; Wang *et al.*, 2016; Domonkos *et al.*, 2017). Therefore, it is possible that symbiosome development was blocked due to the defence/senescence-related responses, which were not sufficiently suppressed. In addition, other studies have shown that arrest of symbiosome development did not induce defence responses (Berrabah *et al.*, 2015), therefore defence is more likely to be a cause than a result of blocking symbiosome development.

Laser capture transcriptome data suggested that *NF-YA1* is highly expressed in the nodule meristem and distal part of infection zone (Roux *et al.*, 2014). Our *in situ* hybridisation data showed that *NF-YA1* was not expressed in the distal part of the meristem, but was expressed at a high level in the proximal part of the meristem and the distal part of the infection zone, where NIN is only present at a very low level. This finding supports the idea that *NF-YA1* expression can be regulated not only by NIN but also by other transcription factor(s).

SymCRK might also be a direct target of NIN as indicated using chromatin immunoprecipitation sequencing (ChIP-seq) analyses on Lotus roots ectopically expressing *NIN* (Soyano *et al.*,

2014; Liu *et al.*, 2019a). In the infection zone, *NIN* is expressed at a very high level, so it could control *SymCRK* expression. If *NIN* also directly controls *SymCRK* expression in the fixation zone, then a very low level of *NIN* might still be sufficient, considering that a low level of *NIN* is sufficient to induce a high level of *NF-YA1* expression. Alternatively, it has been shown that members of the NLP family can also bind to the promoter of *NIN* target gene *CLE-RS2* (Nishida *et al.*, 2018). Moreover, NLPs are highly expressed in *Medicago* nodules, especially MtNLP1/2/3 (Lin *et al.*, 2018), therefore it is possible that they take over the function of *NIN* to maintain expression of this defence suppression gene in the fixation zone.

So, in addition to its function in nodule organogenesis and infection, *NIN* has a major function in establishing a functional symbiosis in *Medicago* nodules. It will be interesting to see whether this function is shared with other legumes or even actinorhizal plants. Such studies in an evolutionary context can provide first insight into when this additional function of *NIN* evolved or whether it is related to a function of the ancestor of *NIN* that was recruited when nodulation evolved.







Acknowledgements

We would like to thank Rebecca Dickstein (University of North Texas) for providing NF10547 (*nin-16*) seeds. This research was supported by the European Research Council (ERC-2011-AdG-294790), and the China Scholarship Council (201506300062 to JL).

Author contributions

JL, OK and TB designed the research. JL, MR and OK performed experiments. JL, MR, TZ, JK, OK and TB analysed data. JL, OK and TB wrote the manuscript.

ORCID

Ton Bisseling  <https://orcid.org/0000-0001-5494-8786>
Joël Klein  <https://orcid.org/0000-0002-0134-5196>
Olga Kulikova  <https://orcid.org/0000-0002-4887-1185>
Jieyu Liu  <https://orcid.org/0000-0001-5607-7291>
Menno Rasing  <https://orcid.org/0000-0001-5025-5130>
Tian Zeng  <https://orcid.org/0000-0002-0315-7658>

References

- Alunni B, Gourion B. 2016. Terminal bacteroid differentiation in the legume–rhizobium symbiosis: nodule-specific cysteine-rich peptides and beyond. *New Phytologist* 211: 411–417.
- Berrabah F, Balliau T, Ait-Salem EH, George J, Zivy M, Ratet P, Gourion B. 2018. Control of the ethylene signaling pathway prevents plant defenses during intracellular accommodation of the rhizobia. *New Phytologist* 219: 310–323.
- Berrabah F, Bourcy M, Cayrel A, Eschstruth A, Mondy S, Ratet P, Gourion B. 2014a. Growth conditions determine the DNF2 requirement for symbiosis. *PLoS ONE* 9: e91866.
- Berrabah F, Bourcy M, Eschstruth A, Cayrel A, Guefrachi I, Mergaert P, Wen J, Jean V, Mysore KS, Gourion B *et al.* 2014b. A nonRD receptor-like kinase prevents nodule early senescence and defense-like reactions during symbiosis. *New Phytologist* 203: 1305–1314.
- Berrabah F, Ratet P, Gourion B. 2015. Multiple steps control immunity during the intracellular accommodation of rhizobia. *Journal of Experimental Botany* 66: 1977–1985.
- Borisov AY, Madsen LH, Tsyganov VE, Umehara Y, Voroshilova VA, Batagov AO, Sandal N, Mortensen A, Schauser L, Ellis N *et al.* 2003. The *Sym35* gene required for root nodule development in pea is an ortholog of *Nin* from *Lotus japonicus*. *Plant Physiology* 131: 1009–1017.
- Bourcy M, Brocard L, Pislariu CI, Cosson V, Mergaert P, Tadege M, Mysore KS, Udvardi MK, Gourion B, Ratet P. 2013. *Medicago truncatula* DNF2 is a PI-PLC-XD-containing protein required for bacteroid persistence and prevention of nodule early senescence and defense-like reactions. *New Phytologist* 197: 1250–1261.
- Bu F, Rutten L, Roswanjaya YP, Kulikova O, Rodriguez-Franco M, Ott T, Bisseling T, van Zeijl A, Geurts R. 2020. Mutant analysis in the nonlegume *Parasponia andersonii* identifies *NIN* and *NF-YA1* transcription factors as a core genetic network in nitrogen-fixing nodule symbioses. *New Phytologist* 226: 541–554.
- Cao H, Qi S, Sun M, Li Z, Yang Y, Crawford NM, Wang Y. 2017. Overexpression of the maize *ZmNLP6* and *ZmNLP8* can complement the arabidopsis nitrate regulatory mutant *nlp7* by restoring nitrate signaling and assimilation. *Frontiers in Plant Science* 8: 1–14.
- Catoira R, Galera C, De Billy F, Penmettsa RV, Journet EP, Maillet F, Rosenberg C, Cook D, Gough C, Denarie J. 2000. Four genes of *Medicago truncatula* controlling components of a Nod factor transduction pathway. *Plant Cell* 12: 1647–1665.
- Chabaud M, Lichtenzweig J, Ellwood S, Pfaff T, Journet P. 2006. Vernalization, crossings and testing for pollen viability. In: Mathesius U, Journet E-P, eds. *Medicago truncatula Handbook*. Ardmore, OK, USA: The Samuel Roberts Noble Foundation, 1–13.
- Clavijo F, Diedhiou I, Vaissayre V, Brottier L, Acolatse J, Moukououanga D, Crabos A, Auguy F, Franche C, Gherbi H *et al.* 2015. The Casuarina *NIN* gene is transcriptionally activated throughout Frankia root infection as well as in response to bacterial diffusible signals. *New Phytologist* 208: 887–903.
- Cruz-Ramírez A, Díaz-Triviño S, Blilou I, Grieneisen VA, Sozzani R, Zamioudis C, Miskolczi P, Nieuwland J, Benjamins R, Dhonukshe P *et al.* 2012. A bistable circuit involving SCARECROW-RETINOBLASTOMA integrates cues to inform asymmetric stem cell division. *Cell* 150: 1002–1015.
- Domonkos Á, Kovács S, Gombár A, Kiss E, Horváth B, Kovács GZ, Farkas A, Tóth MT, Ayaydin F, Bóka K *et al.* 2017. NAD1 controls defense-like responses in *Medicago truncatula* symbiotic nitrogen fixing nodules following rhizobial colonization in a BacA-independent manner. *Genes* 8: 1–21.
- Gavrin A, Kaiser BN, Geiger D, Tyerman SD, Wen Z, Bisseling T, Fedorova EE. 2014. Adjustment of host cells for accommodation of symbiotic bacteria: vacuole defunctionalization, HOPS suppression, and TIP1g retargeting in *medicago*. *Plant Cell* 26: 3809–3822.
- Grandbastien MA. 2015. LTR retrotransposons, handy hitchhikers of plant regulation and stress response. *Biochimica et Biophysica Acta – Gene Regulatory Mechanisms* 1849: 403–416.
- Grandbastien M-A, Spielmann A, Caboche M. 1989. Tnt1, a mobile retroviral-like transposable element of tobacco isolated by plant cell genetics. *Nature* 337: 376–380.
- Grudkowska M, Zagdańska B. 2004. Multifunctional role of plant cysteine proteinases. *Acta Biochimica Polonica* 51: 609–624.
- Guan P, Ripoll J-J, Wang R, Vuong L, Bailey-Steinitz LJ, Ye D, Crawford NM. 2017. Interacting TCP and NLP transcription factors control plant responses to nitrate availability. *Proceedings of the National Academy of Sciences, USA* 114: 2419–2424.
- Haag AF, Balaban M, Sani M, Kerscher B, Pierre O, Farkas A, Longhi R, Boncompagni E, Hérouart D, Dall'Angelo S *et al.* 2011. Protection of *sinorhizobium* against host cysteine-rich antimicrobial peptides is critical for symbiosis. *PLoS Biology* 9: e1001169.
- Hara-Nishimura I, Hatsugai N, Nakaune S, Kuroyanagi M, Nishimura M. 2005. Vacuolar processing enzyme: An executor of plant cell death. *Current Opinion in Plant Biology* 8: 404–408.
- Huisman R, Hontelez J, Mysore KS, Wen J, Bisseling T, Limpens E. 2016. A symbiosis-dedicated SYNTAXIN OF PLANTS 13II isoform controls the

- formation of a stable host-microbe interface in symbiosis. *New Phytologist* 211: 1338–1351.
- Ivanov S, Fedorova EE, Limpens E, De Mita S, Genre A, Bonfante P, Bisseling T. 2012. Rhizobium-legume symbiosis shares an exocytotic pathway required for arbuscule formation. *Proceedings of the National Academy of Sciences, USA* 109: 8316–8321.
- Kulikova O, Franken C, Bisseling T. 2018. *In situ* hybridization method for localization of mRNA molecules in medicago tissue sections. *Methods in Molecular Biology* 1822: 145–159.
- Laporte P, Lepage A, Fournier J, Catrice O, Moreau S, Jardinaud M-F, Mun J-H, Larrainzar E, Cook DR, Gamas P *et al.* 2014. The CCAAT box-binding transcription factor NF-YA1 controls rhizobial infection. *Journal of Experimental Botany* 65: 481–494.
- Limpens E, Ramos J, Franken C, Raz V, Compaan B, Franssen H, Bisseling T, Geurts R. 2004. RNA interference in *Agrobacterium* rhizogenes-transformed roots of *Arabidopsis* and *Medicago truncatula*. *Journal of Experimental Botany* 55: 983–992.
- Lin JS, Li X, Luo ZL, Mysore KS, Wen J, Xie F. 2018. NIN interacts with NLPs to mediate nitrate inhibition of nodulation in *Medicago truncatula*. *Nature Plants* 4: 942–952.
- Liu C, Breakspear A, Guan D, Cerri MR, Jackson K, Jiang S, Robson F, Radhakrishnan GV, Roy S, Bone C *et al.* 2019a. NIN acts as a network hub controlling a growth module required for rhizobial infection. *Plant Physiology* 179: 1704–1722.
- Liu J, Ruten L, Limpens E, van der Molen T, van Velzen R, Chen R, Chen Y, Geurts R, Kohlen W, Kulikova O *et al.* 2019b. A remote *cis*-regulatory region is required for *NIN* expression in the pericycle to initiate nodule primordium formation in *Medicago truncatula*. *Plant Cell* 31: 68–83.
- Liu K, Niu Y, Konishi M, Wu Y, Du H, Chung HS, Li L, Boudsocq M, McCormack M, Maekawa S *et al.* 2017. Discovery of nitrate – CPK – NLP signalling in central nutrient – growth networks. *Nature* 545: 311–316.
- Marchive C, Roudier F, Castaings L, Bréhaut V, Blondet E, Colot V, Meyer C, Krapp A. 2013. Nuclear retention of the transcription factor NLP7 orchestrates the early response to nitrate in plants. *Nature Communications* 4: 1–9.
- Marsh JF, Rakocevic A, Mitra RM, Brocard L, Sun J, Eschstruth A, Long SR, Schultze M, Ratet P, Oldroyd GED. 2007. *Medicago truncatula* *NIN* is essential for rhizobial-independent nodule organogenesis induced by autoactive calcium/calmodulin-dependent protein kinase. *Plant Physiology* 144: 324–335.
- Mergaert P, Nikovics K, Kelemen Z, Maunoury N, Vauvert D, Kondorosi A, Kondorosi E. 2003. A novel family in *Medicago truncatula* consisting of more than 300 nodule-specific genes coding for small, secreted polypeptides with conserved cysteine motifs. *Plant Physiology* 132: 161–173.
- Nishida H, Tanaka S, Handa Y, Ito M, Sakamoto Y, Matsunaga S, Betsuyaku S, Miura K, Soyano T, Kawaguchi M *et al.* 2018. A NIN-LIKE PROTEIN mediates nitrate-induced control of root nodule symbiosis in *Lotus japonicus*. *Nature Communications* 9: 499.
- Oldroyd GED. 2013. Speak, friend, and enter: signalling systems that promote beneficial symbiotic associations in plants. *Nature Reviews Microbiology* 11: 252–263.
- Oldroyd GED, Downie JA. 2008. Coordinating nodule morphogenesis with rhizobial infection in legumes. *Annual Review of Plant Biology* 59: 519–546.
- Oldroyd GED, Murray JD, Poole PS, Downie JA. 2011. The rules of engagement in the legume-rhizobial symbiosis. *Annual Review of Genetics* 45: 119–144.
- Pecrix Y, Staton SE, Sallet E, Lelandais-Brière C, Moreau S, Carrère S, Blein T, Jardinaud M-F, Latrasse D, Zouine M *et al.* 2018. Whole-genome landscape of *Medicago truncatula* symbiotic genes. *Nature Plants* 4: 1017–1025.
- Perez Guerra JC, Coussens G, De Keyser A, De Rycke R, De Bodt S, Van De Velde W, Goormachtig S, Holsters M. 2010. Comparison of developmental and stress-induced nodule senescence in *Medicago truncatula*. *Plant Physiology* 152: 1574–1584.
- Pierre O, Hopkins J, Combiér M, Baldacci F, Engler G, Brouquisse R, Hérouart D, Boncompagni E. 2014. Involvement of papain and legumain proteinase in the senescence process of *Medicago truncatula* nodules. *New Phytologist* 202: 849–863.
- Pislariu CI, Murray JD, Wen J, Cosson V, Muni RR, Wang M, Benedito VA, Andriankaja A, Cheng X, Jerez IT *et al.* 2012. A *Medicago truncatula* tobacco retrotransposon insertion mutant collection with defects in nodule development and symbiotic nitrogen fixation. *Plant Physiology* 159: 1686–1699.
- Roth LE, Stacey G. 1989. Bacterium release into host cells of nitrogen-fixing soybean nodules the symbiosome membrane comes from three sources. *European Journal of Cell Biology* 49: 13–23.
- Roux B, Rodde N, Jardinaud MF, Timmers T, Sauviac L, Cottret L, Carre S, Sallet E, Courcelle E, Moreau S *et al.* 2014. An integrated analysis of plant and bacterial gene expression in symbiotic root nodules using laser-capture microdissection coupled to RNA sequencing. *The Plant Journal* 77: 817–837.
- Saito K, Yonekura-Sakakibara K, Nakabayashi R, Higashi Y, Yamazaki M, Tohge T, Fernie AR. 2013. The flavonoid biosynthetic pathway in *Arabidopsis*: structural and genetic diversity. *Plant Physiology and Biochemistry* 72: 21–34.
- Schauser L, Roussis A, Stiller J, Stougaard J. 1999. A plant regulator controlling development of symbiotic root nodules. *Nature* 402: 191–195.
- Schauser L, Wieloch W, Stougaard J. 2005. Evolution of NIN-like proteins in *Arabidopsis*, rice, and *Lotus japonicus*. *Journal of Molecular Evolution* 60: 229–237.
- Schmid M, Jensen TH. 2008. Quality control of mRNP in the nucleus. *Chromosoma* 117: 419–429.
- Schneider CA, Rasband WS, Eliceiri KW. 2012. NIH Image to ImageJ: 25 years of image analysis. *Nature Methods* 9: 671–675.
- Sheokand S, Brewin NJ. 2003. Cysteine proteases in nodulation and nitrogen fixation. *Indian Journal of Experimental Biology* 41: 1124–1132.
- Sinharoy S, Torres-Jerez I, Bandyopadhyay K, Kereszt A, Pislariu CI, Nakashima J, Benedito VA, Kondorosi E, Udvardi MK. 2013. The C2H2 transcription factor REGULATOR OF SYMBIOSOME DIFFERENTIATION represses transcription of the secretory pathway gene *VAMP721a* and promotes symbiosome development in *Medicago truncatula*. *Plant Cell* 25: 3584–3601.
- Soyano T, Hirakawa H, Sato S, Hayashi M, Kawaguchi M. 2014. Nodule inception creates a long-distance negative feedback loop involved in homeostatic regulation of nodule organ production. *Proceedings of the National Academy of Sciences, USA* 111: 14607–14612.
- Soyano T, Kouchi H, Hirota A, Hayashi M. 2013. NODULE INCEPTION directly targets *NF-Y* subunit genes to regulate essential processes of root nodule development in *Lotus japonicus*. *PLoS Genetics* 9: e1003352.
- Vasse J, De Billy F, Camut S, Truchet G. 1990. Correlation between ultrastructural differentiation of bacteroids and nitrogen fixation in alfalfa nodules. *Journal of Bacteriology* 172: 4295–4306.
- Veerappan V, Jani M, Kadel K, Troiani T, Gale R, Mayes T, Shulaev E, Wen J, Mysore KS, Azad RK *et al.* 2016. Rapid identification of causative insertions underlying *Medicago truncatula* *Tnt1* mutants defective in symbiotic nitrogen fixation from a forward genetic screen by whole genome sequencing. *BMC Genomics* 17: 141.
- Van De Velde W, Guerra JCP, De Keyser A, De Rycke R, Rombauts S, Maunoury N, Mergaert P, Kondorosi E, Holsters M, Goormachtig S. 2006. Aging in legume symbiosis. A molecular view on nodule senescence in *Medicago truncatula*. *Plant Physiology* 141: 711–720.
- Van de Velde W, Zehirov G, Szatmari A, Debreczeny M, Ishihara H, Kevei Z, Farkas A, Mikulass K, Nagy A, Tiricz H *et al.* 2010. Plant peptides govern terminal differentiation of bacteria in symbiosis. *Science* 328: 25–28.
- Vernié T, Kim J, Frances L, Ding Y, Sun J, Guan D, Niebel A, Gifford ML, de Carvalho-Niebel F, Oldroyd GED. 2015. The NIN transcription factor coordinates diverse nodulation programs in different tissues of the *Medicago truncatula* root. *Plant Cell* 27: 3410–3424.
- Vinardell JM, Fedorova E, Cebolla A, Kevei Z, Horvath G, Kelemen Z, Tarayre S, Roudier F, Mergaert P, Kondorosi A *et al.* 2013. Endoreduplication mediated by the anaphase-promoting complex activator CCS52A is required for symbiotic cell differentiation in *Medicago truncatula* nodules. *The Plant Cell* 23: 2093–2105.

- Wagner GP, Kin K, Lynch VJ. 2012. Measurement of mRNA abundance using RNA-seq data: RPKM measure is inconsistent among samples. *Theory in Biosciences* 131: 281–285.
- Wang C, Yu H, Luo L, Duan L, Cai L, He X, Wen J, Mysore KS, Li G, Xiao A *et al.* 2016. NODULES WITH ACTIVATED DEFENSE 1 is required for maintenance of rhizobial endosymbiosis in *Medicago truncatula*. *New Phytologist* 212: 176–191.
- Xiao TT, Schilderink S, Moling S, Deinum EE, Kondorosi E, Franssen H, Kulikova O, Niebel A, Bisseling T. 2014. Fate map of *Medicago truncatula* root nodules. *Development* 141: 3517–3528.
- Xie F, Murray JD, Kim J, Heckmann AB, Edwards A, Oldroyd GED, Downie JA. 2012. Legume pectate lyase required for root infection by rhizobia. *Proceedings of the National Academy of Sciences, USA* 109: 633–638.
- Yu H, Xiao A, Dong R, Fan Y, Zhang X, Liu C, Wang C, Zhu H, Duanmu D, Cao Y *et al.* 2018. Suppression of innate immunity mediated by the CDPK-Rboh complex is required for rhizobial colonization in *Medicago truncatula* nodules. *New Phytologist* 220: 425–434.

Supporting Information

Additional Supporting Information may be found online in the Supporting Information section at the end of the article.

Fig. S1 Expression profile of Medicago NIN/Medtr5g099060 (probe id. Mtr.28094.1.S1.st) based on *M. truncatula* Gene Atlas in various tissues.

Fig. S2 Live/dead staining shows prematurely death of rhizobia in Medicago *nin-16* nodules.

Fig. S3 Medicago *nin-13* mutant nodules show the same phenotype as *nin-16*.

Fig. S4 F1 plants obtained by crossing Medicago *nin-13* and *nin-16* showed the same nodule phenotype as the parental plants.

Fig. S5 *NF-YA1* expression pattern in Medicago *nin-16* nodule.

Fig. S6 *Tnt1* was transcribed in Medicago *nin-13* and *nin-16* mutant nodules.

Fig. S7 *NIN* RNA transcribed from the Medicago *nin-16* allele was altered by *Tnt1* insertion.

Fig. S8 Complementation of Medicago *nin-16* nodule phenotype with *ProNIN*_{3C-5kb}:*NIN*_{ΔPBI} and *ProNIN*_{3C-5kb}:*NIN*.

Table S1 Primers used in this study.

Table S2 Genes with transcripts detected in Medicago *nin-16* or R108 (wild-type).

Table S3 Genes differentially expressed in Medicago *nin-16*.

Table S4 Genes specifically expressed in different Medicago wild-type nodule developmental zones differentially expressed in *nin-16*.

Table S5 Differentially expressed gene families/metabolism pathways in Medicago *nin-16*.

Please note: Wiley Blackwell are not responsible for the content or functionality of any Supporting Information supplied by the authors. Any queries (other than missing material) should be directed to the *New Phytologist* Central Office.